

TIT/HEP-384/NP

August, 1998

Hyperon Non-leptonic Weak Decays in the Chiral Perturbation Theory I

K. Takayama and M. Oka

*Department of Physics, Tokyo Institute of Technology
Meguro, Tokyo 152, Japan*

Hyperon non-leptonic weak decay amplitudes are studied in the chiral perturbation theory. We employ the low energy effective weak Hamiltonian which contains the perturbative QCD correction. To include the non-perturbative QCD effect, quark currents of the effective Hamiltonian are substituted with hadronic currents which are color singlet and are derived by the chiral perturbation theory. We find that the amplitudes caused by the product of hadronic currents are small. It reproduces the small amplitudes of $\Delta I = 3/2$, which are derived by the strong interaction correction.

arXiv:hep-ph/9809388v1 15 Sep 1998

1. Introduction

Hyperon non-leptonic decay amplitudes have been studied very well experimentally[1]; but the corresponding theory is not yet satisfactory[2,3,4,5]. The difficulty comes from that the S- and P-wave amplitudes are not reproduced simultaneously, and that the enhancement mechanism of the $\Delta I = 1/2$ amplitudes is not understood. It is expected that the hyperon decay amplitudes reflect the internal structure of the hyperon and, therefore, QCD corrections to the standard theory must play important roles there. Especially it is difficult to take into account the non-perturbative QCD effect. In order to estimate the amplitudes, low energy effective theories of the hadron are used in the previous study[3].

Chiral perturbation theory is one of the effective theories for the low energy hadron phenomena. The chiral perturbation theory has systematic perturbation on the meson momentum, and is expected to reproduce the low energy hadron phenomena fairly well. But it is known that the chiral perturbation theory cannot reproduce the hyperon non-leptonic weak decay amplitudes. There may remain following questions.

1. What makes it impossible to reproduce the weak interaction in the chiral perturbation theory?
2. Is the chiral perturbation theory enough to describe the strong interaction correction for the weak interaction?

Since the chiral perturbation theory is very useful, it will be applied to more complicated hadron phenomena, for example $Y + N \rightarrow N + N$. It is, therefore, very important to solve above questions.

To consider the role of the chiral perturbation theory, we derive the correction of the weak interaction into two parts, the perturbative QCD corrections and the non-perturbative QCD corrections. The perturbative corrections are taken into account with the one-loop correction to the standard theory, and the low energy effective weak Hamiltonian is derived by using renormalization group method. The effective weak Hamiltonian consists of the products of two quark currents. The non-perturbative QCD corrections are introduced by the chiral perturbation theory. The hyperon and its interaction with pseudo-scalar meson are presented by the heavy baryon formalism of the chiral perturbation theory. In this study, quark currents in the effective weak Hamiltonian are replaced by the hadron currents which are derived from the chiral perturbation theory. The effective weak Hamiltonian is, then, given in terms of the hadron operators. Previously the chiral perturbation theory needs many low energy constants to describe the hyperon non-leptonic weak decay[6]. The parameter fitting with the experimental data is the problem. But, in our method, low energy constants in the effective weak Hamiltonian are derived from the Lagrangian in the strong interaction. This effective weak Hamiltonian demand fewer number of low energy constants. And this Hamiltonian

makes it possible to estimate the $\Delta I = 3/2$ and the $\Delta I = 1/2$ amplitudes separately.

The rest of the paper is organized as follows. Section 2 introduces the effective weak Hamiltonian which includes the perturbative QCD corrections. The effective Hamiltonian described by the hadron operators is constructed in section 3. Section 4 presents the numerical analysis and discussion on the hyperon weak decay amplitudes. Section 5 concludes the paper with the comments on the chiral perturbation theory and the hyperon non-leptonic weak decay amplitudes.

2. The Perturbative QCD Corrections to the Effective Weak Hamiltonian

The hadronic weak interaction is described by the standard theory where the weak bosons are exchanged between quarks[7,8]. The Hamiltonian density of the weak interaction with quarks and weak gauge bosons becomes

$$\mathcal{H}_I(x) = \frac{g}{2\sqrt{2}} J_\mu^+(x) W_\mu^-(x) + \text{H.C.} \quad (2.1)$$

where W^\pm is the charged W -boson field, J_μ^\pm is the charged left-handed current and g is the coupling constant. Eq.(2.1) is applied to the hyperon non-leptonic weak decay. Because the gauge bosons are very heavy, the Hamiltonian for the non-leptonic decay is composed of four quark vertices, which include the QCD correction on the weak vertex. The weak Hamiltonian for the hyperon decay changes the strangeness. The weak transition matrix for $|\Delta S| = 1$ process is defined by[9,10,11]

$$\langle |\mathcal{H}_{eff}^{\Delta S=1}| \rangle = -\frac{i}{2} \int d^4x \langle \text{Tr} \mathcal{H}_I(x) \mathcal{H}_I(0) \rangle \quad (2.2)$$

Using the operator product expansion, it is possible to write the effective Hamiltonian as a sum of four quark operators. The coefficients of the operator depend on the mass scale. At the scale $\mu = M_W$ the QCD running coupling constant α_s is small, the coefficients can be expanded perturbatively in α_s . Paschos et al.[11] deduced the following effective Hamiltonian at $\mu = M_W$:

$$\mathcal{H}_{eff}^{\Delta S=1} |_{\mu=M_W} = \frac{G_f}{\sqrt{2}} \left[\xi_u (\bar{d}_\alpha u_\alpha) (\bar{u}_\beta s_\beta) + \xi_c (\bar{d}_\alpha c_\alpha) (\bar{c}_\beta s_\beta) \right] + \mathcal{H}_{penguin}^{top}, \quad (2.3)$$

where α, β denote the color index. ξ_q satisfies $\xi_q \equiv V_{qd}^* V_{qs}$ where V is the Cabibbo-Kobayashi-Maskawa matrix[13]. The first term is the pure weak interaction where the transferred momentum is lower than the W -boson mass scale. This term has the $\Delta I = 3/2$ component as well as the $\Delta I = 1/2$ component. The second term represents the one-loop QCD correction caused by the top quark in the internal line, which is called as penguin diagram. Since the top quark is heavier than the W -boson, this second term is treated separately. The scale μ in eq. (2.3) is changed with the renormalization group method, and the effective Hamiltonian

for the low mass scale are obtained, where one-loop QCD correction are taken into account perturbatively. In this calculation, the renormalization scale μ is changed to $\mu^2 \simeq \mu_0^2$ where $\alpha(\mu_0^2) = 1$ is satisfied, as is prescribed in Bardeen et al.[14]. The effective weak Hamiltonian becomes

$$H_{eff}^{\Delta S=1}(\mu^2 \approx \mu_0^2) = -\frac{G_f}{\sqrt{2}} \sum_{r=1}^6 K_r O_r, \quad (2.4)$$

where the operators O_r are given by

$$\begin{aligned} O_1 &= (\bar{d}_\alpha s_\alpha)_{V-A} (\bar{u}_\beta u_\beta)_{V-A} - (\bar{u}_\alpha s_\alpha)_{V-A} (\bar{d}_\beta u_\beta)_{V-A} \\ O_2 &= (\bar{d}_\alpha s_\alpha)_{V-A} (\bar{u}_\beta u_\beta)_{V-A} + (\bar{u}_\alpha s_\alpha)_{V-A} (\bar{d}_\beta u_\beta)_{V-A} \\ &\quad + 2(\bar{d}_\alpha s_\alpha)_{V-A} (\bar{d}_\beta d_\beta)_{V-A} + 2(\bar{d}_\alpha s_\alpha)_{V-A} (\bar{s}_\beta s_\beta)_{V-A} \\ O_3 \left(\Delta I = \frac{1}{2} \right) &= \frac{1}{3} \left[(\bar{d}_\alpha s_\alpha)_{V-A} (\bar{u}_\beta u_\beta)_{V-A} + (\bar{u}_\alpha s_\alpha)_{V-A} (\bar{d}_\beta u_\beta)_{V-A} \right. \\ &\quad \left. + 2(\bar{d}_\alpha s_\alpha)_{V-A} (\bar{d}_\beta d_\beta)_{V-A} - 3(\bar{d}_\alpha s_\alpha)_{V-A} (\bar{s}_\beta s_\beta)_{V-A} \right] \\ O_4 \left(\Delta I = \frac{3}{2} \right) &= \frac{5}{3} \left[(\bar{d}_\alpha s_\alpha)_{V-A} (\bar{u}_\beta u_\beta)_{V-A} + (\bar{u}_\alpha s_\alpha)_{V-A} (\bar{d}_\beta u_\beta)_{V-A} \right. \\ &\quad \left. - (\bar{d}_\alpha s_\alpha)_{V-A} (\bar{d}_\beta d_\beta)_{V-A} \right] \\ O_5 &= (\bar{d}_\alpha s_\alpha)_{V-A} (\bar{u}_\beta u_\beta + \bar{d}_\beta d_\beta + \bar{s}_\beta s_\beta)_{V+A} \\ O_6 &= (\bar{d}_\alpha s_\beta)_{V-A} (\bar{u}_\beta u_\alpha + \bar{d}_\beta d_\alpha + \bar{s}_\beta s_\alpha)_{V+A}. \end{aligned} \quad (2.5)$$

The coefficients $K_r (r = 1, \dots, 6)$ are obtained from the calculation of the Wilson coefficients and the Cabibbo-Kobayashi-Maskawa matrix elements. Two types of the Wilson coefficients are adopted for the comparison, whose conditions are $m_t = 200[\text{GeV}]$, $\mu_0 = 0.24[\text{GeV}]$, $\Lambda^{(4)} = 0.10[\text{GeV}]$ and $m_t = 200[\text{GeV}]$, $\mu_0 = 0.71[\text{GeV}]$, $\Lambda^{(4)} = 0.316[\text{GeV}]$. The coefficients are listed in Table 2.1. In both cases, μ_0 is defined so as to satisfy $\alpha_s(\mu^2) = 1$. The operators are described as a sum of products of the $SU(3)_f$ currents. Since each current belongs to the $SU(3)_f$ octet representation, the effective weak Hamiltonian belongs to the **8** or **27** dimensional representation. In eq.(2.5) the operator O_3 and O_4 belong to the **27** representation. Only the operator O_4 has the $\Delta I = 3/2$ component, and other operators have only $\Delta I = 1/2$ component. The Wilson coefficients in eq.(2.4) suggest the enhancement of the $\Delta I = 1/2$ amplitudes, but it is known that this perturbative enhancement is not enough[12]. The correction using the renormalization group method does not contain full effect of the QCD correction to calculate the amplitudes of non-leptonic weak decays of hyperons. At the low momentum, the soft gluons are exchanged between quarks, which causes the non-perturbative effect. The estimation of the non-perturbative effect is very important for the hyperon weak decay. It is, therefore, necessary to introduce a low energy effective model which includes non-perturbative effects of QCD.

3. Chiral Effective Weak Hamiltonian for Hyperon Decays

3.1. CHIRAL PERTURBATION THEORY IN HEAVY BARYON FORMALISM

Chiral perturbation theory treats hadrons as elementary fields[15,16]. The hadron properties can be calculated by perturbative expansions with respect to hadron momenta, quark masses and baryon mass differences[17,18]. The chiral perturbation is valid if the momentum k is sufficiently smaller than the chiral symmetry breaking scale $\Lambda_\chi \sim 1[\text{GeV}]$. In the same way the quark mass matrix $M = \text{diag}(m_u, m_d, m_s)$ is suppressed by a factor m/Λ_χ .

The chiral Lagrangian is constructed with these expansions, requiring the chiral invariance, Lorentz invariance and parity conservation. The lowest and next order chiral Lagrangians for meson fields are given by

$$\mathcal{L}_2 = \frac{f_\pi^2}{4} \text{Tr}\{(\mathcal{D}_\mu \Sigma)(\mathcal{D}^\mu \Sigma^\dagger) + \chi \Sigma^\dagger + \Sigma \chi^\dagger\}, \quad (3.1)$$

$$\begin{aligned} \mathcal{L}_4 = & L_1(\text{Tr}\{\mathcal{D}_\mu \Sigma \mathcal{D}^\mu \Sigma^\dagger\})^2 + L_2(\text{Tr}\{\mathcal{D}_\mu \Sigma D_\nu \Sigma^\dagger\} \text{Tr}\{\mathcal{D}^\mu \Sigma D^\nu \Sigma^\dagger\}) \\ & + L_3 \text{Tr}\{\mathcal{D}_\mu \Sigma \mathcal{D}^\mu \Sigma^\dagger D_\nu \Sigma D^\nu \Sigma^\dagger\} + L_4(\text{Tr}\{\mathcal{D}_\mu \Sigma \mathcal{D}^\mu \Sigma^\dagger\} \text{Tr}\{\chi \Sigma^\dagger + \Sigma \chi^\dagger\}) \\ & + L_5 \text{Tr}\{\mathcal{D}_\mu \Sigma \mathcal{D}^\mu \Sigma^\dagger (\chi \Sigma^\dagger + \Sigma \chi^\dagger)\} + L_6(\text{Tr}\{\chi \Sigma^\dagger + \Sigma \chi^\dagger\})^2 \\ & + L_7(\text{Tr}\{\chi \Sigma^\dagger - \Sigma \chi^\dagger\})^2 + L_8 \text{Tr}\{\Sigma \chi^\dagger \Sigma \chi^\dagger + \chi \Sigma^\dagger \chi \Sigma^\dagger\} \\ & - iL_9 \text{Tr}\{F_R^{\mu\nu} \mathcal{D}_\mu \Sigma D_\nu \Sigma^\dagger + F_L^{\mu\nu} \mathcal{D}_\mu \Sigma^\dagger D_\nu \Sigma\} + L_{10} \text{Tr}\{\Sigma F_R^{\mu\nu} \Sigma^\dagger F_{\mu\nu}^L\} \\ & + H_1 \text{Tr}\{F_R^{\mu\nu} F_{\mu\nu}^R + F_L^{\mu\nu} F_{\mu\nu}^L\} + H_2 \text{Tr}\{\chi \chi^\dagger\}, \end{aligned} \quad (3.2)$$

where $L_1 \sim L_{10}$ are the coupling constants. These values are determined phenomenologically and are shown in Table 3.1. The meson field $\Sigma(x)$ is given by

$$\Sigma(x) = \xi^2(x) = e^{2i\pi(x)/f_\pi}, \quad \xi(x) = e^{i\pi(x)/f_\pi}. \quad (3.3)$$

This field is transformed under $SU(3)_L \times SU(3)_R$ as $\Sigma \longrightarrow L \Sigma R^\dagger$. In order to preserve the local chiral invariance, the external gauge fields \mathcal{V}_μ and \mathcal{A}_μ appear through covariant derivative of mesons

$$\begin{aligned} \mathcal{D}_\mu \Sigma &= \partial_\mu \Sigma - i(\mathcal{V}_\mu + \mathcal{A}_\mu) \Sigma + i \Sigma (\mathcal{V}_\mu - \mathcal{A}_\mu) \\ \mathcal{D}_\mu \Sigma^\dagger &= \partial_\mu \Sigma^\dagger + i \Sigma^\dagger (\mathcal{V}_\mu + \mathcal{A}_\mu) - i(\mathcal{V}_\mu - \mathcal{A}_\mu) \Sigma^\dagger, \end{aligned} \quad (3.4)$$

and through the field strength tensors

$$\begin{aligned} F_L^{\mu\nu} &= \partial_\mu (\mathcal{V}_\nu - \mathcal{A}_\nu) - \partial_\nu (\mathcal{V}_\mu - \mathcal{A}_\mu) - i [(\mathcal{V}_\mu - \mathcal{A}_\mu), (\mathcal{V}_\nu - \mathcal{A}_\nu)] \\ F_R^{\mu\nu} &= \partial_\mu (\mathcal{V}_\nu + \mathcal{A}_\nu) - \partial_\nu (\mathcal{V}_\mu + \mathcal{A}_\mu) - i [(\mathcal{V}_\mu + \mathcal{A}_\mu), (\mathcal{V}_\nu + \mathcal{A}_\nu)]. \end{aligned} \quad (3.5)$$

The external scalar and pseudo-scalar fields, \mathcal{S} and \mathcal{P} respectively, are introduced as $\chi = 2B_0(\mathcal{S} - i\mathcal{P})$ and $\chi^\dagger = 2B_0(\mathcal{S} + i\mathcal{P})$, where the quark mass matrix M is included in S . Under the $SU(3)_L \times SU(3)_R$ chiral symmetry, these external fields have the following transformations,

$$\begin{aligned} (\mathcal{S} + i\mathcal{P}) &\longrightarrow R(\mathcal{S} + i\mathcal{P})L^\dagger \\ (\mathcal{S} - i\mathcal{P}) &\longrightarrow L(\mathcal{S} - i\mathcal{P})R^\dagger \\ (\mathcal{V}_\mu - \mathcal{A}_\mu) &\longrightarrow L(\mathcal{V}_\mu - \mathcal{A}_\mu)L^\dagger + iL(\partial_\mu L^\dagger) \\ (\mathcal{V}_\mu + \mathcal{A}_\mu) &\longrightarrow R(\mathcal{V}_\mu + \mathcal{A}_\mu)R^\dagger + iR(\partial_\mu R^\dagger). \end{aligned} \quad (3.6)$$

We follow the heavy baryon formulation for the octet and decuplet baryons. Introducing the four-velocity v_μ , the momentum p_μ of the baryon becomes[17]

$$p_\mu = m_B v_\mu + k_\mu \quad (3.7)$$

where m_B is the average octet baryon mass and k_μ represents the residual off-shell momentum of the baryon interacting with Goldstone bosons. In the heavy baryon formalism, the first term in eq.(3.7) is removed and momentum expansion can be treated in the same way as the Goldstone bosons. The mass term expansion gives power series of $1/m_B$.

Using the expansions, the lowest order chiral Lagrangian for baryon fields is given by[18]

$$\begin{aligned} \mathcal{L}_v^{(1)} = & i\text{Tr}\bar{B}_v(v \cdot \mathcal{D})B_v + 2D\text{Tr}\bar{B}_v S_v^\mu \{A_\mu, B_v\} + 2F\text{Tr}\bar{B}_v S_v^\mu [A_\mu, B_v] \\ & - i\bar{T}_v^\mu (v \cdot \mathcal{D})T_{v\mu} + \mathcal{C} \left(\bar{T}_v^\mu A_\mu B_v + \bar{B}_v A_\mu T_v^\mu \right) + 2\mathcal{H}\bar{T}_v^\mu S_{v\nu} A^\nu T_{v\mu} \\ & + \Delta m \bar{T}_v^\mu T_{v\mu}, \end{aligned} \quad (3.8)$$

where D , F , \mathcal{H} and \mathcal{C} are the coupling constants determined phenomenologically. The decuplet-octet mass difference is $\Delta m = m_T - m_B$. The lowest order Lagrangian coupled to the scalar and pseudo-scalar external fields is given by

$$\begin{aligned} \mathcal{L}_v^{(2)} = & a_1 \text{Tr}\bar{B}_v \{(\xi^\dagger \chi \xi^\dagger + \xi \chi^\dagger \xi), B_v\} + a_2 \text{Tr}\bar{B}_v [(\xi^\dagger \chi \xi^\dagger + \xi \chi^\dagger \xi), B_v] \\ & + a_3 \text{Tr}\bar{B}_v B_v \text{Tr}(\xi^\dagger \chi \xi^\dagger + \xi \chi^\dagger \xi) \\ & + c_1 \bar{T}_v^\mu (\xi^\dagger \chi \xi^\dagger + \xi \chi^\dagger \xi) T_{v\mu} + c_2 \bar{T}_v^\mu T_{v\mu} \text{Tr}(\xi^\dagger \chi \xi^\dagger + \xi \chi^\dagger \xi). \end{aligned} \quad (3.9)$$

The velocity dependent baryon fields are defined by

$$\begin{aligned} B_v(x) &= \frac{1+\not{v}}{2} e^{im_B \not{v} \cdot x} B(x), \\ T_v^\mu(x) &= \frac{1+\not{v}}{2} e^{im_B \not{v} \cdot x} T^\mu(x), \end{aligned} \quad (3.10)$$

where B and T correspond to the octet and decuplet baryon fields, respectively. The decuplet baryon fields are represented by the Rarita-Schwinger field T_μ^{abc} which contains both Lorentz index μ and spinor indices a, b, c . This field satisfies a constraint $v^\mu \cdot T_{v\mu}^{abc} = 0$. The velocity dependent field have the two component spinors which are derived from the four component spinors by the projection. The Dirac gamma matrix γ^μ of the baryon-pion couplings in the Lagrangian is replaced by the velocity vector v_μ and $\gamma^\mu \gamma^5$ by the velocity dependent spinor operator S_v^μ [17,18].

The fields are transformed under $SU(3)_L \times SU(3)_R$ symmetry as

$$\begin{aligned} B &\longrightarrow U(x) B U(x)^\dagger \\ T_{abc}^\mu &\longrightarrow U_a^d U_b^e U_c^f T_{def}^\mu, \end{aligned} \quad (3.11)$$

where $U(x)$ is defined by $\xi(x) \longrightarrow L\xi(x)U^\dagger(x) = U(x)\xi(x)R^\dagger$. The Lagrangian $\mathcal{L}^{(1)}$ represents the pions derivatively coupled to the octet and decuplet baryons through the vector and axial-vector fields,

$$\bar{V}^\mu = \frac{1}{2} \left(\xi \partial^\mu \xi^\dagger + \xi^\dagger \partial^\mu \xi \right), \quad \bar{A}^\mu = \frac{i}{2} \left(\xi \partial^\mu \xi^\dagger - \xi^\dagger \partial^\mu \xi \right). \quad (3.12)$$

In order to preserve the local chiral invariance, the external gauge fields \mathcal{V}^μ appears through covariant derivative

$$\begin{aligned}\mathcal{D}^\mu B_v &= \partial^\mu B_v + [V^\mu, B_v] \\ \mathcal{D}^\mu T_v^\nu &= \partial^\mu T_{abc}^\nu + (V^\mu)_a^d T_{dbc}^\nu + (V^\mu)_b^d T_{adc}^\nu + (V^\mu)_c^d T_{abd}^\nu,\end{aligned}\tag{3.13}$$

where V^μ is defined by

$$V^\mu \equiv \bar{V}^\mu - \frac{i}{2}\xi^\dagger (\mathcal{V}^\mu - \mathcal{A}^\mu) \xi - \frac{i}{2}\xi (\mathcal{V}^\mu + \mathcal{A}^\mu) \xi^\dagger.\tag{3.14}$$

And the external gauge field \mathcal{A}^μ appears through the interaction term

$$\begin{aligned}\mathcal{L}_{v\ int}^{(1)} &= 2D\text{Tr}\bar{B}_v S_v^\mu \{A_\mu, B_v\} + 2F\text{Tr}\bar{B}_v S_v^\mu [A_\mu, B_v] \\ &\quad + \mathcal{C} \left(\bar{T}_v^\mu A_\mu B_v + \bar{B}_v A_\mu T_v^\mu \right) + 2\mathcal{H}\bar{T}_v^\mu S_{v\nu} A^\nu T_{v\mu}\end{aligned}\tag{3.15}$$

where A^μ is defined by

$$A^\mu \equiv \bar{A}^\mu - \frac{i}{2}\xi^\dagger (\mathcal{V}^\mu - \mathcal{A}^\mu) \xi - \frac{i}{2}\xi (\mathcal{V}^\mu + \mathcal{A}^\mu) \xi^\dagger.\tag{3.16}$$

We apply the chiral Lagrangian (3.1), (3.2), (3.8) and (3.9) to derive the effective weak Hamiltonian for the hyperon decay.

3.2. CHIRAL EFFECTIVE HAMILTONIAN FOR WEAK INTERACTION

The low energy effective weak Hamiltonian (2.4) is given as a sum of products of two quark currents. Hence, it is natural to construct an effective hadronic weak Hamiltonian by substituting the quark currents by hadron currents, term by term. But the quark operators can not be replaced by the hadronic operators directly, since the hadronic operators do not have the same property as the quark operators. As the effective weak Hamiltonian includes all the hyperon decay processes, we, therefore, introduce the following three ansatz.

1. Fierz transformation is applied to the four quark operators, and the form of the four quark operators are changed.
2. The effective weak Hamiltonian is constructed by summing up all the weak operators which are derived by the Fierz transformation.
3. The quark currents are replaced by the hadronic currents which have the same symmetry under the chiral transformation.

For the first ansatz, the Fierz transformation is applied to the quark currents and they become

$$\begin{aligned}\left(\bar{d}_\alpha u_\alpha\right)_{V-A} \left(\bar{u}_\beta s_\beta\right)_{V-A} &\longrightarrow \frac{1}{3} \left(\bar{u}_\alpha u_\alpha\right)_{V-A} \left(\bar{d}_\beta s_\beta\right)_{V-A} \\ \left(\bar{d}_\alpha s_\beta\right)_{V-A} \left(\bar{u}_\beta u_\alpha\right)_{V+A} &\longrightarrow -\frac{32}{9} \left(\bar{d}_\alpha u_\alpha\right)_{S-iP} \left(\bar{u}_\beta s_\beta\right)_{S+iP}.\end{aligned}\tag{3.17}$$

Summing up all the operators, eq.(2.5) becomes

$$\begin{aligned}
O_1 &= \frac{2}{3} \left[(\bar{d}_\alpha s_\alpha)_{V-A} (\bar{u}_\beta u_\beta)_{V-A} - (\bar{u}_\alpha s_\alpha)_{V-A} (\bar{d}_\beta u_\beta)_{V-A} \right] \\
O_2 &= \frac{4}{3} \left[(\bar{d}_\alpha s_\alpha)_{V-A} (\bar{u}_\beta u_\beta)_{V-A} + (\bar{u}_\alpha s_\alpha)_{V-A} (\bar{d}_\beta u_\beta)_{V-A} \right. \\
&\quad \left. + 2(\bar{d}_\alpha s_\alpha)_{V-A} (\bar{d}_\beta d_\beta)_{V-A} + 2(\bar{d}_\alpha s_\alpha)_{V-A} (\bar{s}_\beta s_\beta)_{V-A} \right] \\
O_3 \left(\Delta I = \frac{1}{2} \right) &= \frac{4}{9} \left[(\bar{d}_\alpha s_\alpha)_{V-A} (\bar{u}_\beta u_\beta)_{V-A} + (\bar{u}_\alpha s_\alpha)_{V-A} (\bar{d}_\beta u_\beta)_{V-A} \right. \\
&\quad \left. + 2(\bar{d}_\alpha s_\alpha)_{V-A} (\bar{d}_\beta d_\beta)_{V-A} - 3(\bar{d}_\alpha s_\alpha)_{V-A} (\bar{s}_\beta s_\beta)_{V-A} \right] \\
O_4 \left(\Delta I = \frac{3}{2} \right) &= \frac{20}{9} \left[(\bar{d}_\alpha s_\alpha)_{V-A} (\bar{u}_\beta u_\beta)_{V-A} + (\bar{u}_\alpha s_\alpha)_{V-A} (\bar{d}_\beta u_\beta)_{V-A} \right. \\
&\quad \left. - (\bar{d}_\alpha s_\alpha)_{V-A} (\bar{d}_\beta d_\beta)_{V-A} \right] \\
O_5 &= O_{51} + O_{52} \\
O_{51} &= (\bar{d}_\alpha s_\alpha)_{V-A} (\bar{u}_\beta u_\beta + \bar{d}_\beta d_\beta + \bar{s}_\beta s_\beta)_{V+A} \\
O_{52} &= -\frac{2}{3} \left[(\bar{d}_\alpha u_\alpha)_{S+iP} (\bar{u}_\beta u_\beta)_{S-iP} + (\bar{d}_\alpha d_\alpha)_{S+iP} (\bar{d}_\beta s_\beta)_{S-iP} \right. \\
&\quad \left. + (\bar{d}_\alpha s_\alpha)_{S+iP} (\bar{s}_\beta s_\beta)_{S-iP} \right] \\
O_6 &= O_{60} + O_{61} \\
O_{60} &= (\bar{d}_\alpha s_\beta)_{V-A} (\bar{u}_\beta u_\alpha + \bar{d}_\beta d_\alpha + \bar{s}_\beta s_\alpha)_{V+A} \\
O_{61} &= -\frac{32}{9} \left[(\bar{d}_\alpha u_\alpha)_{S+iP} (\bar{u}_\beta s_\beta)_{S-iP} + (\bar{d}_\alpha d_\alpha)_{S+iP} (\bar{d}_\beta s_\beta)_{S-iP} \right. \\
&\quad \left. + (\bar{d}_\alpha s_\alpha)_{S+iP} (\bar{s}_\beta s_\beta)_{S-iP} \right].
\end{aligned} \tag{3.18}$$

The operator O_{52} and O_{61} include $S \pm iP$ currents. The operator O_{60} have the color non-singlet current. Therefore the operator O_{60} cannot be replaced by the product of the hadronic currents.

Next we derive the hadronic currents for the third ansatz. Consider an extended QCD Lagrangian coupling to external Hermitian matrix valued fields \mathcal{V}_μ , \mathcal{A}_μ , \mathcal{S}_μ and \mathcal{P}_μ ;

$$\mathcal{L}_{QCD} = \mathcal{L}_{QCD}^0 + \bar{q} \gamma^\mu (\mathcal{V}_\mu + \gamma_5 \mathcal{A}_\mu) q - \bar{q}_R (\mathcal{S} - i\mathcal{P}) q_L - \bar{q}_L (\mathcal{S} + i\mathcal{P}) q_R. \tag{3.19}$$

The chiral Lagrangian and the QCD Lagrangian which can describe the same hadron phenomena are connected via the external fields. We derive the hadron operator currents by taking appropriate derivatives with respect to the external fields;

$$\begin{aligned}
\mathcal{J}_{L\mu}^{ij} &= \frac{\partial \mathcal{L}}{\partial (\mathcal{V}_\mu - \mathcal{A}_\mu)} = \bar{q}_i \gamma_\mu (1 - \gamma_5) q_j \\
&= \text{Tr} v_\mu \bar{B}_v \left[\xi^\dagger h_{ij} \xi, B_v \right] - 2D \text{Tr} \bar{B}_v S_{v\mu} \left\{ \xi^\dagger h_{ij} \xi, B_v \right\} \\
&\quad - 2F \text{Tr} \bar{B}_v S_{v\mu} \left[\xi^\dagger h_{ij} \xi, B_v \right] \\
&\quad - v_\mu \bar{T}_v^\nu \left(\xi^\dagger h_{ij} \xi \right) T_{v\nu} - 2\mathcal{H} \bar{T}_v^\nu S_{v\mu} \left(\xi^\dagger h_{ij} \xi \right) T_{v\nu} \\
&\quad - 2\mathcal{C} \left(\bar{T}_{v\mu} \left(\xi^\dagger h_{ij} \xi \right) B_v + \bar{B}_v \left(\xi^\dagger h_{ij} \xi \right) T_{v\mu} \right) \\
&\quad + i f_\pi^2 \text{Tr} \left(h_{ij} (\partial_\mu \Sigma) \Sigma^\dagger \right),
\end{aligned} \tag{3.20}$$

$$\begin{aligned}
\mathcal{J}_{R\mu}^{ij} &= \frac{\partial \mathcal{L}}{\partial (\mathcal{V}_\mu + \mathcal{A}_\mu)} = \bar{q}_i \gamma_\mu (1 + \gamma_5) q_j \\
&= \text{Tr} v_\mu \bar{B}_v \left[\xi h_{ij} \xi^\dagger, B_v \right] + 2D \text{Tr} \bar{B}_v S_{v\mu} \left\{ \xi h_{ij} \xi^\dagger, B_v \right\} \\
&\quad + 2F \text{Tr} \bar{B}_v S_{v\mu} \left[\xi h_{ij} \xi^\dagger, B_v \right] \\
&\quad - v_\mu \bar{T}_v^\nu \left(\xi h_{ij} \xi^\dagger \right) T_{v\nu} + 2\mathcal{H} \bar{T}_v^\nu S_{v\mu} \left(\xi h_{ij} \xi^\dagger \right) T_{v\nu} \\
&\quad + 2\mathcal{C} \left(\bar{T}_{v\mu} \left(\xi h_{ij} \xi^\dagger \right) B_v + \bar{B}_v \left(\xi h_{ij} \xi^\dagger \right) T_{v\mu} \right) \\
&\quad + i f_\pi^2 \text{Tr} \left(h_{ij} (\partial_\mu \Sigma^\dagger) \Sigma \right), \tag{3.21}
\end{aligned}$$

$$\mathcal{J}_{(S+iP)}^{ij} = \mathcal{J}_{0(S+iP)}^{ij} + \mathcal{J}_{2(S+iP)}^{ij} = \frac{\partial \mathcal{L}}{\partial (\mathcal{S} + iP)} = \bar{q}_i (1 + \gamma_5) q_j \tag{3.22}$$

$$\begin{aligned}
\mathcal{J}_{0(S+iP)}^{ij} &= a_1 \text{Tr} \bar{B}_v \left\{ \xi^\dagger h_{ij} \xi^\dagger, B_v \right\} + a_2 \text{Tr} \bar{B}_v \left[\xi^\dagger h_{ij} \xi^\dagger, B_v \right] \\
&\quad + a_3 \text{Tr} \left(\bar{B}_v B_v \right) \text{Tr} \left(\xi^\dagger h_{ij} \xi^\dagger \right) \\
&\quad + c_1 \bar{T}_v^\mu \left(\xi^\dagger h_{ij} \xi^\dagger \right) T_{v\mu} + c_2 \bar{T}_v^\mu T_{v\mu} \text{Tr} \left(\xi^\dagger h_{ij} \xi^\dagger \right) \\
&\quad + \frac{f_\pi^2}{2} B_0 \text{Tr} \left(h_{ij} \Sigma^\dagger \right) \tag{3.23}
\end{aligned}$$

$$\begin{aligned}
\mathcal{J}_{2(S+iP)}^{ij} &= 2B_0 L_4 \text{Tr} \left(\mathcal{D}_\mu \Sigma \mathcal{D}^\mu \Sigma^\dagger \right) \text{Tr} \left(h_{ij} \Sigma^\dagger \right) \\
&\quad + 2B_0 L_5 \text{Tr} \left(h_{ij} \mathcal{D}_\mu \Sigma \mathcal{D}^\mu \Sigma^\dagger \Sigma^\dagger \right), \tag{3.24}
\end{aligned}$$

$$\mathcal{J}_{(S-iP)}^{ij} = \mathcal{J}_{0(S-iP)}^{ij} + \mathcal{J}_{2(S-iP)}^{ij} = \frac{\partial \mathcal{L}}{\partial (\mathcal{S} - iP)} = \bar{q}_i (1 - \gamma_5) q_j \tag{3.25}$$

$$\begin{aligned}
\mathcal{J}_{0(S-iP)}^{ij} &= a_1 \text{Tr} \bar{B}_v \left\{ \xi h_{ij} \xi, B_v \right\} + a_2 \text{Tr} \bar{B}_v \left[\xi h_{ij} \xi, B_v \right] \\
&\quad + a_3 \text{Tr} \left(\bar{B}_v B_v \right) \text{Tr} \left(\xi h_{ij} \xi \right) \\
&\quad + c_1 \bar{T}_v^\mu \left(\xi h_{ij} \xi \right) T_{v\mu} + c_2 \bar{T}_v^\mu T_{v\mu} \text{Tr} \left(\xi h_{ij} \xi \right) \\
&\quad + \frac{f_\pi^2}{2} B_0 \text{Tr} \left(h_{ij} \Sigma \right) \tag{3.26}
\end{aligned}$$

$$\begin{aligned}
\mathcal{J}_{2(S-iP)}^{ij} &= 2B_0 L_4 \text{Tr} \left(\mathcal{D}_\mu \Sigma \mathcal{D}^\mu \Sigma^\dagger \right) \text{Tr} \left(h_{ij} \Sigma \right) \\
&\quad + 2B_0 L_5 \text{Tr} \left(h_{ij} \mathcal{D}_\mu \Sigma \mathcal{D}^\mu \Sigma^\dagger \Sigma \right), \tag{3.27}
\end{aligned}$$

where h is the 3×3 matrix satisfying the relation

$$(h_{ij})_{ab} = \begin{cases} 1 & a = i \text{ and } b = j \\ 0 & \text{others.} \end{cases} \tag{3.28}$$

These currents are transformed under chiral transform as follows,

$$\mathcal{J}_L : h_{ij} \longrightarrow L h_{ij} L^\dagger \quad (8_L, 1_R)$$

$$\begin{aligned}
\mathcal{J}_R : h_{ij} &\longrightarrow Rh_{ij}R^\dagger & (1_L, 8_R) \\
\mathcal{J}_{(S+iP)} : h_{ij} &\longrightarrow Lh_{ij}R^\dagger & (3_L, \bar{3}_R) \\
\mathcal{J}_{(S-iP)} : h_{ij} &\longrightarrow Rh_{ij}L^\dagger & (\bar{3}_L, 3_R).
\end{aligned}$$

Because $\mathcal{J}_{L\mu}^{ij}$ and $\mathcal{J}_{R\mu}^{ij}$ are the Noether currents, which are conserved, they are not renormalized, while the scalar and pseudo-scalar currents, which are not conserved, may be renormalized.

Substituting the quark bilinears in the operators (3.18) by hadronic currents, we obtain a hadronic representation of the weak Hamiltonian,

$$\mathcal{H}_{eff}^{\Delta S=1} = -\frac{G_f}{\sqrt{2}} \sum_{r=1}^6 K_r O_r. \quad (3.29)$$

The effective weak operators are given by

$$\begin{aligned}
O_1 &= \frac{2}{3} \left(\mathcal{J}_{L\mu}^{23} \mathcal{J}_L^{11\mu} - \mathcal{J}_{L\mu}^{13} \mathcal{J}_L^{21\mu} \right) \\
O_2 &= \frac{4}{3} \left(\mathcal{J}_{L\mu}^{23} \mathcal{J}_L^{11\mu} + \mathcal{J}_{L\mu}^{13} \mathcal{J}_L^{21\mu} + 2\mathcal{J}_{L\mu}^{23} \mathcal{J}_L^{22\mu} + 2\mathcal{J}_{L\mu}^{23} \mathcal{J}_L^{33\mu} \right) \\
O_3 &= O_3 (\Delta I = 1/2) \\
&= \frac{4}{9} \left(\mathcal{J}_{L\mu}^{23} \mathcal{J}_L^{11\mu} + \mathcal{J}_{L\mu}^{13} \mathcal{J}_L^{21\mu} + 2\mathcal{J}_{L\mu}^{23} \mathcal{J}_L^{22\mu} - 3\mathcal{J}_{L\mu}^{23} \mathcal{J}_L^{33\mu} \right) \\
O_4 &= O_3 (\Delta I = 3/2) \\
&= \frac{20}{9} \left(\mathcal{J}_{L\mu}^{23} \mathcal{J}_L^{11\mu} + \mathcal{J}_{L\mu}^{13} \mathcal{J}_L^{21\mu} - \mathcal{J}_{L\mu}^{21} \mathcal{J}_L^{22\mu} \right) \\
O_5 &= O_{51} + O_{52} + O_{53} \\
O_{51} &= \left(\mathcal{J}_{L\mu}^{23} \mathcal{J}_R^{11\mu} + \mathcal{J}_{L\mu}^{23} \mathcal{J}_R^{22\mu} + \mathcal{J}_{L\mu}^{23} \mathcal{J}_R^{33\mu} \right) \\
O_{52} &= -\frac{2}{3} \left(\mathcal{J}_{0(S+iP)}^{21} \mathcal{J}_{0(S-iP)}^{13} + \mathcal{J}_{0(S+iP)}^{22} \mathcal{J}_{0(S-iP)}^{23} + \mathcal{J}_{0(S+iP)}^{23} \mathcal{J}_{0(S-iP)}^{33} \right) \\
O_{53} &= -\frac{2}{3} \left(\mathcal{J}_{2(S+iP)}^{21} \mathcal{J}_{0(S-iP)}^{13} + \mathcal{J}_{0(S+iP)}^{21} \mathcal{J}_{2(S-iP)}^{13} + \mathcal{J}_{2(S+iP)}^{22} \mathcal{J}_{0(S-iP)}^{23} \right. \\
&\quad \left. + \mathcal{J}_{0(S+iP)}^{22} \mathcal{J}_{2(S-iP)}^{23} + \mathcal{J}_{2(S+iP)}^{23} \mathcal{J}_{0(S-iP)}^{33} + \mathcal{J}_{0(S+iP)}^{23} \mathcal{J}_{2(S-iP)}^{33} \right) \\
O_6 &= O_{61} + O_{62} \\
O_{61} &= -\frac{32}{9} \left(\mathcal{J}_{0(S+iP)}^{21} \mathcal{J}_{0(S-iP)}^{13} + \mathcal{J}_{0(S+iP)}^{22} \mathcal{J}_{0(S-iP)}^{23} + \mathcal{J}_{0(S+iP)}^{23} \mathcal{J}_{0(S-iP)}^{33} \right) \\
O_{62} &= -\frac{32}{9} \left(\mathcal{J}_{2(S+iP)}^{21} \mathcal{J}_{0(S-iP)}^{13} + \mathcal{J}_{0(S+iP)}^{21} \mathcal{J}_{2(S-iP)}^{13} + \mathcal{J}_{2(S+iP)}^{22} \mathcal{J}_{0(S-iP)}^{23} \right. \\
&\quad \left. + \mathcal{J}_{0(S+iP)}^{22} \mathcal{J}_{2(S-iP)}^{23} + \mathcal{J}_{2(S+iP)}^{23} \mathcal{J}_{0(S-iP)}^{33} + \mathcal{J}_{0(S+iP)}^{23} \mathcal{J}_{2(S-iP)}^{33} \right)
\end{aligned} \quad (3.30)$$

The coefficients K_r are given in Table 2.1.

In this study the effective Hamiltonian is constructed within chiral order $\mathcal{O}(p^2)$. The quark condensation term has chiral order $\mathcal{O}(p^0)$. In order to have the consistent chiral ordering to the effective Hamiltonian, the next-to leading order $\mathcal{O}(p^2)$ of the scalar and pseudo-scalar currents are needed. Therefore, the currents $\mathcal{J}_{(S+iP)}^{ij}$, $\mathcal{J}_{(S-iP)}^{ij}$ are divided into $\mathcal{J}_{0(S+iP)}^{ij}$, $\mathcal{J}_{2(S+iP)}^{ij}$ and $\mathcal{J}_{0(S-iP)}^{ij}$, $\mathcal{J}_{2(S-iP)}^{ij}$, respectively. The operators O_5 and O_6 in eq.(3.18) are represented by $O_{51} + O_{52} + O_{53}$ and $O_{61} + O_{62}$, respectively. The constants a_1 , a_2 , a_3 , c_1 and c_2 are determined by the comparison between the computation of the chiral perturbation theory and experimental data.

The above effective weak Hamiltonian includes only the interaction between color singlet hadron currents which is shown in Fig. 3.1(a). There is a weak interaction that four quark

vertex appears in the hyperon, which is shown in Fig. 3.1(b). It corresponds to the two point vertex of the baryon operator in chiral perturbation theory. It is not enough to extract all the effects of this interaction by the factorization method from eq. (3.17). Therefore other terms have to be introduced to the effective weak Hamiltonian. These terms have the many coupling constants which are determined by the experimental data. In order to clear the hadronic currents effect of the weak Hamiltonian, we adopt the simple effective weak Hamiltonian (3.29). The effect of the two point vertex of the baryon operator in the chiral perturbation theory is discussed in ref.[23,24]. It is also noted that the weak interaction shown in Fig. 3.1(b) do not affect the $\Delta I = 3/2$ amplitudes according to the Pati and Woo theorem[21]. Hence the $\Delta I = 3/2$ amplitudes are appear only in the operator O_4 and we can analyze them. In the following, we calculate the hyperon non-leptonic weak decay amplitudes with the effective Hamiltonian (3.29).

4. Hyperon Non-leptonic Weak Decays

4.1. NUMERICAL ANALYSIS

Non-leptonic weak decay amplitude is conventionally defined by the following formula[1].

$$\mathcal{M}(B_i \longrightarrow B_f + \pi) = G_F m_{\pi^+}^2 \bar{u}_f (A + B \gamma_5) u_i, \quad (4.1)$$

where A is the S-wave amplitude and B is the P-wave one. In the heavy baryon formalism the decay amplitude is given by

$$\mathcal{M}(B_i \longrightarrow B_f + \pi) = \frac{G_f}{\sqrt{2}} \bar{U}_f (\mathcal{A} + (q \cdot S_v) \mathcal{B}) U_i, \quad (4.2)$$

where q is the momentum of outgoing pion. Note that G_F and G_f are the Fermi coupling constants but have different values: $G_F = 10^{-5} m_p^{-2}$, $G_f = 1.166 \times 10^{-11} [\text{MeV}^{-2}]$. In the heavy baryon formalism, the baryons have the two component spinors, while baryons in eq. (4.1) are described by four component spinors. In the rest frame of the initial baryon, the two component spinors are extracted from eq. (4.1), and we obtain the following relations between decay amplitudes,

$$\begin{aligned} A &= \frac{-iG_f}{\sqrt{2}G_F m_{\pi^+}^2} f_{\pi} \mathcal{A} \\ B &= \frac{iG_f}{2\sqrt{2}G_F m_{\pi^+}^2} (E_f + m_f) f_{\pi} \mathcal{B}, \end{aligned} \quad (4.3)$$

where E_f is the energy of the final baryon and m_f is the final state baryon mass. The hyperon non-leptonic weak decays are measured for the following seven processes:

$$\begin{aligned} \Sigma^- &\longrightarrow n + \pi^- \quad (\Sigma_-^-), \quad \Sigma^+ \longrightarrow n + \pi^+ \quad (\Sigma_+^+), \quad \Sigma^+ \longrightarrow p + \pi^0 \quad (\Sigma_0^+), \\ \Lambda &\longrightarrow n + \pi^0 \quad (\Lambda_0^0), \quad \Lambda \longrightarrow p + \pi^- \quad (\Lambda_-^0), \quad \Xi^- \longrightarrow \Lambda + \pi^- \quad (\Xi_-^-), \quad \Xi^0 \longrightarrow \Lambda + \pi^0 \quad (\Xi_0^0). \end{aligned}$$

There are 14 measured amplitudes since each 7 decay process have the S- and P-wave amplitudes.

Using the strong interaction Lagrangian (3.1), (3.2), (3.8) and the effective weak Hamiltonian (3.29), the S- and P-wave hyperon non-leptonic decay amplitudes are calculated. The tree level amplitudes are obtained from the calculation of Feynman diagrams in Fig. 4.1. Since the diagrams (2), (3) and (4) have a strong interaction vertex ($q \cdot S_v$), these diagrams cause only P-wave decay amplitudes. The chiral logarithmic terms in the one-loop correction are obtained from the calculation of Feynman diagrams in Fig. 4.2. The S-wave amplitudes are obtained from Fig. 4.2 (9), (10), (11), (30), (35), (40), (41), (42), (43), (44), (45), (48). The rest of diagrams and (40), (41), (42), (43), (44), (45) contribute to the chiral logarithmic terms of the P-wave amplitudes. The wave function renormalization is applied to the internal and external lines of hadrons. Examples of the wave function renormalization are shown in Fig. 4.3. The amplitudes are given by the summation of these diagrams. In our study the wave function renormalization for the intermediate baryon and meson are taken into account. The tree level amplitudes are given by

S-wave:

$$\begin{aligned}
A(\Sigma^-) &= 3.0705 \times 10^{-1} - 2.3337 \times 10^{-1}a_1 + 2.3337 \times 10^{-1}a_2 \\
A(\Sigma_+^+) &= 0 \\
A(\Sigma_0^+) &= -7.0563 \times 10^{-2} + 1.6502 \times 10^{-1}a_1 - 1.6502 \times 10^{-1}a_2 \\
A(\Lambda_0^0) &= -6.3084 \times 10^{-2} - 6.7368 \times 10^{-2}a_1 - 2.0210 \times 10^{-1}a_2 \\
A(\Lambda_-^-) &= 2.7450 \times 10^{-1} + 9.5273 \times 10^{-2}a_1 + 2.8582 \times 10^{-1}a_2 \\
A(\Xi_-^-) &= -3.1012 \times 10^{-1} + 9.5273 \times 10^{-2}a_1 - 2.8582 \times 10^{-1}a_2 \\
A(\Xi_0^0) &= 7.1268 \times 10^{-2} - 6.7368 \times 10^{-2}a_1 + 2.0210 \times 10^{-1}a_2
\end{aligned} \tag{4.4}$$

P-wave:

$$\begin{aligned}
B(\Sigma^-) &= 2.2212 + 1.2058a_1 + 8.2856 \times 10^{-1}a_2 \\
B(\Sigma_+^+) &= -1.9490a_1 + 3.9833a_2 \\
B(\Sigma_0^+) &= -1.2804 - 2.2308a_1 + 2.2308a_2 \\
B(\Lambda_0^0) &= 4.4732 - 1.1459 \times 10^{-1}a_1 - 2.7816a_2 \\
B(\Lambda_-^-) &= -7.7599 + 1.6205 \times 10^{-1}a_1 + 3.9338a_2 \\
B(\Xi_-^-) &= 3.0086 - 1.8612a_1 - 2.7488a_2 \\
B(\Xi_0^0) &= -1.7343 + 1.3161a_1 + 1.9437a_2
\end{aligned} \tag{4.5}$$

The tree level amplitudes and the chiral logarithmic terms in the one-loop correction are given by

S-wave:

$$\begin{aligned}
A(\Sigma^-) &= 3.2554 \times 10^1 + 3.0862 \times 10^1a_1 - 3.1032 \times 10^1a_2 - 2.5229 \times 10^{-2}c_1 \\
A(\Sigma_+^+) &= -6.0803 - 1.0944 \times 10^{-4}a_1 + 6.7828 \times 10^{-3}a_2 \\
A(\Sigma_0^+) &= -1.5360 \times 10^1 - 2.1816 \times 10^1a_1 + 2.1951 \times 10^1a_2 + 1.7840 \times 10^{-2}c_1 \\
A(\Lambda_0^0) &= -3.1614 \times 10^{-1} + 8.8775a_1 + 2.6754 \times 10^1a_2 + 1.0109 \times 10^{-1}c_1 \\
A(\Lambda_-^-) &= 2.5155 - 1.2557 \times 10^1a_1 - 3.7855 \times 10^1a_2 - 1.4297 \times 10^{-1}c_1 \\
A(\Xi_-^-) &= -2.4018 \times 10^1 - 1.2758 \times 10^1a_1 + 3.7914 \times 10^1a_2 + 5.3009 \times 10^{-2}c_1 \\
A(\Xi_0^0) &= 1.1550 \times 10^1 + 9.0225a_1 - 2.6800 \times 10^1a_2 - 3.7483 \times 10^{-2}c_1
\end{aligned} \tag{4.6}$$

P-wave:

$$\begin{aligned}
B(\Sigma^-) &= 6.9622 \times 10^2 + 2.2896 \times 10^1 a_1 + 2.3957 \times 10^1 a_2 + 8.3649 a_3 - 5.4327 \times 10^{-1} c_1 \\
B(\Sigma^+_\dagger) &= 1.4794 \times 10^2 - 3.2295 \times 10^2 a_1 + 2.8974 \times 10^2 a_2 - 7.2823 \times 10^{-1} c_1 \\
B(\Sigma^+_0) &= -3.8548 \times 10^2 - 2.4455 \times 10^2 a_1 + 1.8794 \times 10^2 a_2 - 5.9149 a_3 - 1.3079 \times 10^{-1} c_1 \\
B(\Lambda^0_0) &= 1.7307 \times 10^3 - 7.6621 \times 10^1 a_1 - 3.2130 \times 10^2 a_2 + 1.6514 \times 10^1 a_3 - 5.3588 \times 10^{-1} c_1 \\
B(\Lambda^0_-) &= -2.4466 \times 10^3 + 1.0836 \times 10^2 a_1 + 4.5438 \times 10^2 a_2 - 2.3354 \times 10^1 a_3 + 7.5786 \times 10^{-1} c_1 \\
B(\Xi^-) &= 9.6124 \times 10^2 - 2.9146 \times 10^2 a_1 - 3.0700 \times 10^2 a_2 + 9.9536 a_3 - 3.8293 \times 10^{-1} c_1 \\
B(\Xi^0_0) &= -6.8022 \times 10^2 + 2.0609 \times 10^2 a_1 + 2.1708 \times 10^2 a_2 - 7.0383 a_3 + 2.7077 \times 10^{-1} c_1
\end{aligned} \tag{4.7}$$

In this computation, following hadron masses and constants are used:

$$\begin{aligned}
m_n &= 939[\text{MeV}], & m_\Sigma &= 1193[\text{MeV}], & m_\Lambda &= 1116[\text{MeV}] \\
m_\Xi &= 1318[\text{MeV}], & m_\Delta &= 1232[\text{MeV}], & m_{\Sigma^*} &= 1385[\text{MeV}] \\
m_{\Xi^*} &= 1533[\text{MeV}], & m_\Omega &= 1672[\text{MeV}] \\
M_\pi &= 138[\text{MeV}], & M_K &= 496[\text{MeV}], & M_\eta &= 547[\text{MeV}] \\
D &= 0.61, & F &= 0.40, & \mathcal{C} &= 1.6 \\
\mathcal{H} &= -1.9, & f_\pi &= 93[\text{Mev}], & L_4 &= -0.3003 \\
L_5 &= 1.399, & B_0 &= 1391.4[\text{MeV}],
\end{aligned} \tag{4.8}$$

data set 2.

And for the chiral logarithmic terms, the renormalization scale $4\pi\mu^2 = 1.0 \times 10^6 [\text{MeV}^2]$ is used. The amplitudes have 4 unknown parameters, a_1 , a_2 , a_3 and c_1 . The constants a_1 and a_2 that appear in the scalar current are determined as $a_1 = 29.1/m_s$ and $a_2 = -94.8/m_s$ where m_s is the strange quark mass. They are derived from the baryon mass difference with the chiral perturbation theory[22]. The remaining two parameters are fitted with 14 experimental data. The amplitudes derived from fitted parameters are shown in Table 4.1. The fitted parameters are shown in Table 4.2. Constant terms in eq. (4.6) and (4.7) have large values, which are caused by the quark condensation value B_0 . The decay amplitudes depend on the quark condensation value strongly. To reproduce the experimental data, the quark condensation value is changed as $B_0 = 1.3914 \times 10^3 [\text{MeV}]$, $1.3914 \times 10^2 [\text{MeV}]$, $0.0 [\text{MeV}]$. Since the Table 4.1 shows that amplitudes extracted with data set 2 and $B_0 = 1.3914 \times 10^2 [\text{MeV}]$ have better fitting with experimental data, we adopt these parameters in the following analysis. From the Table 2.1, the difference between data set 1 and 2 are large in K_5 and K_6 . This difference is responsible for the amplitudes caused by the operators O_5 and O_6 . The components of the predicted amplitudes are shown in Table 4.3. The operators O_{52} , O_{53} , O_{61} and O_{62} which include the scalar and pseudo-scalar currents are proportional to the quark condensation value B_0 . If we adopt the condition $B_0 = 0.0 [\text{MeV}]$, The amplitudes do not depend on the parameters a_1 , a_2 , a_3 and c_1 . The components of these amplitudes are shown in Table 4.4. These tables suggest that the contributions of the chiral logarithmic correction are large. The tree level amplitudes caused by each operator in eq. (3.30) are shown in Table 4.5 and the

chiral logarithmic amplitudes caused by each operator are shown in Table 4.6.

4.2. DISCUSSION

Table 4.1 shows that the amplitudes derived by the hadronic current interaction do not reproduce the experimental data well. It is caused by the lack of two point vertex of the baryon operator and by uncertainties of the quark condensation in scalar and pseudo-scalar currents. If we choose the condition $B_0 = 0.0[\text{MeV}]$, the contributions of the scalar and pseudo-scalar currents become zero. The amplitudes are, therefore, caused by the $V \pm A$ current interaction in the operator O_1, O_2, O_3, O_4 and O_{51} . Table 4.1 shows that the S-wave amplitudes Σ_-^-, Λ_-^0 and Ξ_-^- are almost caused by the $V \pm A$ currents. In the other amplitudes the contributions of the scalar, pseudo-scalar currents and two point vertex of the baryon operator are large.

Table 4.3 and 4.4 show the large amplitudes caused by the chiral logarithmic correction. In the chiral order analysis, the logarithmic correction of the one-loop diagram has the order of magnitude, $\frac{M_K^2}{16\pi^2 f_\pi^2} \ln\left(\frac{M_K^2}{4\pi\mu^2}\right) \approx 0.20$. The effect of the one-loop calculation expected to be 25% correction to tree level amplitudes. But there are many loop diagrams which have many internal baryon states. Since the amplitudes are obtained by the summation of all diagrams, the amplitudes caused by the loop correction become large.

Let us considering the contribution of the each operator. In the tree level the operator O_1 is most important for the amplitudes, which is shown in Table 4.5. Since the tree level amplitudes do not depend on the free parameters a_3 and c_1 , these amplitudes depend on B_0 value and they are small. The amplitudes caused by the two point vertex of the baryon operator must be large. But in the chiral logarithmic correction, the operators composed of the scalar and pseudo-scalar currents become important. Especially the weak Hamiltonian caused by meson currents, which is shown in Fig.4.2 (9), (10) etc., is important since these terms are proportional to B_0^2 and sensitive to the B_0 value. In order to reproduce the experimental data by the chiral perturbation theory, it is important to construct the O_5 and O_6 operators exactly.

In our method $\Delta I = 3/2$ amplitudes are derived from the operator O_4 and it does not depend on the unknown coupling constant in the chiral perturbation theory. In the tree level, the S-wave $\Delta I = 3/2$ amplitudes are given by the diagram (1) in Fig.4.1 and the P-wave amplitudes are given by the diagrams (1) and (4) in Fig.4.1. The chiral logarithmic corrections of the S-wave $\Delta I = 3/2$ amplitudes are obtained from the diagrams (9), (10), (11), (30), (35), (40), (41) and (48) in Fig.4.2, and the P-wave amplitudes are obtained from the diagrams (1)~(8), (26)~(29), (31)~(34), (36)~(41) and (48) in Fig.4.2. The comparison between the experimental data and the calculated data with our method are shown in Table 4.7. In the tree level, the absolute values of the $\Delta I = 3/2$ amplitudes become small. It is consistent to the $\Delta I = 1/2$ rule. These small amplitudes are caused by the small coupling constants $F, D < 1$ in the chiral perturbation theory. But including the chiral logarithmic correction

of the one-loop diagrams, the amplitudes become large. These amplitudes are caused by the summation of the many logarithmic term in loop diagrams and by the large coupling constants $|\mathcal{H}|, \mathcal{C} > 1$ of the decuplet fields.

5. Conclusion

Hyperon non-leptonic weak decay amplitudes are studied by the chiral perturbation theory. Applying the renormalization method to the weak interaction, the effective weak Hamiltonian which has perturbative QCD correction is obtained. The effective weak Hamiltonian is described by the quark bilinear form. These quark currents are substituted by the hadronic currents derived by the chiral perturbation theory.

Our results suggest that the color singlet $V \pm A$ current interaction has the small contribution to the decay amplitudes. The weak interaction caused by the scalar, pseudo-scalar currents and by the two point vertex of the baryon operator have the large contribution. The $\Delta I = 3/2$ amplitudes are suppressed. Using the chiral perturbation theory as the strong interaction correction for the weak interaction, it is consistent to the experimental data. Our method have no parameters for the $\Delta I = 3/2$ amplitudes. Applying our method to the more complicated decay process, like $Y + N \rightarrow N + N$, it is possible to predict the characteristic of the $\Delta I = 3/2$ amplitudes.

In order to reproduce the experimental data quite well, it is necessary to study the two point vertex of the baryon operator, the quark condensation value B_0 for the weak interaction and the relation between the renormalization scale μ of the perturbative QCD correction and the chiral perturbation theory.

References

- [1] Review of Particle Properties, Phys. Lett. **B111** (1982) 286
- [2] J. Bijnens, H. Sonoda and M. B. Wise, Nucl. Phys. **B261** (1985) 185
- [3] J. F. Donoghue, E. Golowich and B. Holstein, Phys. Rep. **131** (1986) 319
- [4] E. Jenkins, Nucl. Phys. **B375** (1992) 561
- [5] R. Springer, preprint DUKE-95-95
- [6] B. Borasoy and B. R. Holstein ,”Non-leptonic Hyperon Decays in Chiral Perturbation Theory” hep-ph/9805430
- [7] S. Weinberg, Phys. Rev. Lett. **19** (1967) 1264,
A. Salam : in Elementary Particle Theory ed. by N. Svartholom
- [8] D. Bailin, “Weak Interaction”, (Adam Hilger LTD, Bristol, 1982)
- [9] A. I. Valnshtein, V. I. Zakharov and M. A. Shifman JETP **45** ('77) 670
- [10] F. J. Gilman and M. B. Wise, Phys. Rev. **D20** (1979) 2392
- [11] E. A. Paschos, T. Schneider and Y. L. Wu, Nucl. Phys. **B332** (1990) 285
- [12] L. B. Okun, Leptons and Quarks (North-Holland, Netherland, 1982)
- [13] M. Kobayashi and T. Maskawa, Prog. Theor. Phys. **49** (1973) 652
- [14] W. A. Bardeen, A. J. Buras and J.-M. Gerard, Phys. Lett. **B192** (1987) 138
W. A. Bardeen, A. J. Buras and J.-M. Gerard, Nucl. Phys. **B293** (1987) 787
- [15] J. Gasser and H. Leutwyler Ann. Phys. (N.Y.) **158** (1984) 142; Nucl. Phys. **B250** (1985) 465; Nucl. Phys. **B250** (1985) 517; Nucl. Phys. **B250** (1985) 539
- [16] S. Weinberg, Physica **96A** (1979) 327
- [17] E. Jenkins and A. V. Manohar, Phys. Lett. **B255** (1991) 558
- [18] E. Jenkins and A. V. Manohar, Phys. Lett. **B259** (1991) 353
- [19] J. Bijnens and F. Cornet, Nucl. Phys. **B296** (1988) 557
- [20] J. Bijnens, G. Ecker and J. Gasser, in :The DAFNE Physics Handbook (vol. 1), eds. L. Maiani, G. Pancheri and N. Paver, INFN Frascati, 1992
- [21] J. C. Pati and C. H. Woo, Phys. Rev. **D3** (1971) 2920
- [22] E. Jenkins, Nucl. Phys. **B368** (1992) 190
- [23] K. Takayama, Thesis, Tokyo Institute of Technology 1997
- [24] in preparation

Table 2.1 The values of the coefficients in the effective weak Hamiltonian (2.4). The values are taken from Ref.[11]. The data set 1 corresponds to the choices $m_t = 200[\text{GeV}]$ and $\mu_0 = 0.24[\text{GeV}]$, $\Lambda_{QCD} = 0.10$. The data set 2 corresponds to the choices $m_t = 200[\text{GeV}]$ and $\mu_0 = 0.71[\text{GeV}]$, $\Lambda_{QCD} = 0.316$. In both cases, μ_0 is defined so as to satisfy $\alpha_s(\mu^2) = 1$.

	data set 1	data set 2
$\mu(\text{GeV})$	0.24	0.71
$\Lambda^{(4)}(\text{GeV})$	0.10	0.316
K_1	-0.284	-0.270
K_2	0.009	0.011
K_3	0.026	0.027
K_4	0.026	0.027
K_5	0.004	0.002
K_6	0.004	0.002

Table 3.1 Phenomenological values of the renormalized couplings $L_i^r(M_\rho)$. $L_i^r(i = 4, \dots, 8)$ are from ref.[15], $L_{9,10}^r$ from ref.[19] and $L_{1,2,3}^r$ from ref.[20].

i	$L_i^r(M_\rho)$
1	0.7 ± 0.5
2	1.2 ± 0.4
3	-3.6 ± 1.3
4	-0.3 ± 0.5
5	1.4 ± 0.5
6	-0.2 ± 0.3
7	-0.4 ± 0.15
8	0.9 ± 0.3
9	6.9 ± 0.2
10	-5.2 ± 0.3

Table 4.1 The tree and one-loop level amplitudes. First column corresponds to the experimental data. The quark condensation value B_0 is varied as $B_0 = 1.3914 \times 10^3[\text{MeV}]$, $B_0 = 1.3914 \times 10^2[\text{MeV}]$ and $B_0 = 0.0[\text{MeV}]$.

S-wave:

decay mode	exp.	data set 1			data set 2		
		1.3941×10^3	1.3941×10^2	0.0	1.3941×10^3	1.3941×10^2	0.0
Σ^-	1.93 ± 0.01	93.06	6.157	1.732	45.32	4.016	1.717
Σ^+	0.06 ± 0.01	-12.75	-0.1616	-0.03402	-6.082	-0.09894	-0.03831
Σ_0^+	-1.48 ± 0.05	-50.80	-3.278	-0.2901	-24.39	-1.805	-0.2463
Λ_0^0	-1.07 ± 0.02	-14.24	-6.484	-0.5509	-7.790	-4.1018	-0.4985
Λ_0^-	1.47 ± 0.01	23.13	10.35	1.938	13.09	7.012	1.907
Ξ^-	-2.04 ± 0.01	-75.01	-7.689	-2.173	-37.17	-5.175	-2.142
Ξ_0^0	1.54 ± 0.03	42.63	4.480	0.6749	20.85	2.719	0.6203

P-wave:

decay mode	exp.	data set 1			data set 2		
		1.3941×10^3	1.3941×10^2	0.0	1.3941×10^3	1.3941×10^2	0.0
Σ^-	-0.65 ± 0.07	-433.8	-3.070	2.304	-204.2	0.5967	2.316
Σ^+	19.07 ± 0.07	31.33	15.84	7.479	24.19	16.83	7.216
Σ_0^+	12.04 ± 0.58	330.8	15.75	6.038	163.7	13.95	5.935
Λ_0^0	-7.14 ± 0.56	128.9	-4.52	-0.5050	58.51	-4.901	-0.4810
Λ_0^-	9.98 ± 0.24	-179.9	6.079	0.3647	-81.83	6.581	0.3174
Ξ^-	6.93 ± 0.31	-71.30	1.399	0.4604	-34.72	-0.1677	0.4341
Ξ_0^0	-6.43 ± 0.66	49.51	-1.167	-0.4958	24.02	-0.06164	-0.4837

Table 4.2 The parameters of scalar and pseudo-scalar currents. Two types of data set are used. Fixing the B_0 value, we obtain eq. (4.4), (4.5), (4.6) and (4.7). The parameters are fitted with least square method.

parameter	dataset 1		
B_0	1.3914×10^3	1.3914×10^2	0.0
a_1	1.9400×10^{-1}	1.9400×10^{-1}	-
a_2	-6.3200×10^{-1}	-6.3200×10^{-1}	-
a_3	-1.0652×10^2	-2.3960×10^1	-
c_1	8.9337	-2.0402×10^2	-

parameter	dataset 2		
B_0	1.3914×10^3	1.3914×10^2	0.0
a_1	1.9400×10^{-1}	1.9400×10^{-1}	-
a_2	-6.3200×10^{-1}	-6.3200×10^{-1}	-
a_3	-1.0692×10^2	-2.7993×10^1	-
c_1	1.1855	-2.8150×10^2	-

Table 4.3 The predicted amplitudes with $B_0 = 1.3941 \times 10^2[\text{MeV}]$, data set 2 and the parameters in Table 4.2. A_{exp} and B_{exp} correspond to the experimental data. A_{tree} and B_{tree} are the tree level amplitudes. ΔA_{loop} and ΔB_{loop} are the summation of the chiral logarithmic correction of the one-loop graphs. They are represented with $\Delta A_{loop} = \Delta A_{octet} + \Delta A_{decuplet}$ and $\Delta B_{loop} = \Delta B_{octet} + \Delta B_{decuplet}$. A_{theory} and B_{theory} are the total amplitude of the chiral perturbation theory, which are represented with $A_{theory} = A_{tree} + \Delta A_{loop}$ and $B_{theory} = B_{tree} + \Delta B_{loop}$.

S-wave:

decay mode	$A_{exp.}$	A_{theory}	A_{tree}	ΔA_{loop}	ΔA_{octet}	$\Delta A_{decuplet}$
Σ^-	1.93 ± 0.01	4.016	0.2974	3.719	1.739	1.980
Σ^+	0.06 ± 0.01	-0.09894	0.0	-0.09894	-0.04420	-0.05474
Σ_0^+	-1.48 ± 0.05	-1.805	-0.06375	-1.741	-1.149	-0.5920
Λ_0^0	-1.07 ± 0.02	-4.102	-0.05735	-4.044	-0.6702	-3.374
Λ_0^-	1.47 ± 0.01	7.012	0.2664	6.746	1.619	5.127
Ξ^-	-2.04 ± 0.01	-5.175	-0.3002	-4.875	-1.880	-2.995
Ξ_0^-	1.54 ± 0.03	2.719	0.06423	2.655	1.109	1.546

P-wave:

decay mode	$B_{exp.}$	B_{theory}	B_{tree}	ΔB_{loop}	ΔB_{octet}	$\Delta B_{decuplet}$
Σ^-	-0.65 ± 0.07	0.5967	0.6097	-0.01300	-17.31	17.29
Σ^+	19.07 ± 0.07	16.83	-0.1448	16.98	-11.31	28.29
Σ_0^+	12.04 ± 0.58	13.95	-0.2433	14.19	4.578	9.615
Λ_0^0	-7.14 ± 0.56	-4.901	0.6148	-5.516	-19.30	13.79
Λ_0^-	9.98 ± 0.24	6.581	-2.303	8.885	26.22	-17.34
Ξ^-	6.93 ± 0.31	-0.1677	0.9142	-1.081	-10.93	9.851
Ξ_0^-	-6.43 ± 0.66	-0.06164	-0.2534	0.1917	8.392	-8.200

Table 4.4 The predicted amplitudes with $B_0 = 0.0[\text{MeV}]$, data set 2. A_{exp} and B_{exp} correspond to the experimental data. A_{tree} and B_{tree} are the tree level amplitudes. ΔA_{loop} and ΔB_{loop} are the summation of the chiral logarithmic correction of the one-loop graphs. They are represented with $\Delta A_{loop} = \Delta A_{octet} + \Delta A_{decuplet}$ and $\Delta B_{loop} = \Delta B_{octet} + \Delta B_{decuplet}$. A_{theory} and B_{theory} are the total amplitude of the chiral perturbation theory, which are represented with $A_{theory} = A_{tree} + \Delta A_{loop}$ and $B_{theory} = B_{tree} + \Delta B_{loop}$.

S-wave:

decay mode	$A_{exp.}$	A_{theory}	A_{tree}	ΔA_{loop}	ΔA_{octet}	$\Delta A_{decuplet}$
Σ^-	1.93 ± 0.01	1.717	0.3071	1.410	0.3558	1.054
Σ^+	0.06 ± 0.01	-0.03831	0.0	-0.03831	-0.04977	0.01146
Σ_0^+	-1.48 ± 0.05	-0.2463	-0.07056	-0.1757	-0.2162	0.04050
Λ_0^0	-1.07 ± 0.02	-0.4985	-0.06308	-0.4354	0.07263	-0.5080
Λ_0^-	1.47 ± 0.01	1.907	0.2745	1.633	0.5580	1.075
Ξ^-	-2.04 ± 0.01	-2.142	-0.3101	-1.832	-0.4793	-1.353
Ξ_0^-	1.54 ± 0.03	0.6203	0.07127	0.5490	0.1440	0.4050

P-wave:

decay mode	$B_{exp.}$	B_{theory}	B_{tree}	ΔB_{loop}	ΔB_{octet}	$\Delta B_{decuplet}$
Σ^-	-0.65 ± 0.07	2.316	0.6080	1.708	-0.6232	2.331
Σ^+	19.07 ± 0.07	7.216	0.0	7.216	-0.02100	7.237
Σ_0^+	12.04 ± 0.58	5.935	-0.1397	6.075	0.7635	5.312
Λ_0^0	-7.14 ± 0.56	-0.4810	0.4882	-0.9692	0.06545	-1.035
Λ_0^-	9.98 ± 0.24	0.3174	-2.124	2.442	-1.179	3.621
Ξ^-	6.93 ± 0.31	0.4341	0.8236	-0.3894	0.6008	-0.9902
Ξ_0^-	-6.43 ± 0.66	-0.4837	-0.1893	-0.2945	0.2395	-0.5340

Table 4.5 The amplitudes for each operator in the tree level calculation with data set 2 and $B_0 = 1.3914 \times 10^2 [\text{MeV}]$. The first column corresponds to the operator number of the effective Hamiltonian (3.29) and (3.30). The second row shows the observed data.

S-wave:

vertex	Σ_-^-	Σ_+^+	Σ_0^+	Λ_0^0	Λ_-^0	Ξ_-^-	Ξ_0^-
exp.	1.93	0.06	-1.48	-1.07	1.47	-2.04	-1.54
O_1	0.2073	0	-0.1466	-0.1310	0.1853	-0.2093	0.1480
O_2	0.01689	0	-0.01194	-0.01068	0.01510	-0.01706	0.01206
O_3	0.01382	0	-0.009770	-0.008735	0.01235	-0.01396	0.009868
O_4	0.06909	0	0.09770	0.08735	0.06176	-0.06978	-0.09868
O_{51}	0	0	0	0	0	0	0
O_{52}	3.755E-4	0	-2.655E-4	-2.234E-4	3.159E-4	-3.879E-4	2.743E-4
O_{53}	0	0	0	0	0	0	0
O_{61}	-0.01001	0	0.007081	0.005956	-0.008424	0.01034	-0.007314
O_{62}	0	0	0	0	0	0	0

P-wave:

vertex	Σ_-^-	Σ_+^+	Σ_0^+	Λ_0^0	Λ_-^0	Ξ_-^-	Ξ_0^-
exp.	-0.65	19.07	12.04	-7.14	9.98	6.93	-6.43
O_1	0.4104	0	-0.2902	1.01387	-1.434	0.5559	-0.3931
O_2	0.03344	0	-0.02365	0.08261	-0.1168	0.04530	-0.03203
O_3	0.02736	0	-0.01935	0.06759	-0.09559	0.03706	-0.02621
O_4	0.1368	0	0.1935	-0.6759	-0.4779	0.1853	0.2621
O_{51}	0	0	0	0	0	0	0
O_{52}	6.199E-4	0.005641	0.003550	-0.003244	0.004588	-0.002606	0.001842
O_{53}	-6.840E-4	0	4.837E-4	-0.001690	0.002390	-9.265E-4	6.551E-4
O_{61}	-0.01653	-0.1504	-0.09467	0.08651	-0.1223	0.06948	-0.04913
O_{62}	0.01824	0	-0.01290	0.04506	-0.06373	0.02471	-0.01747

Table 4.6 The amplitudes for each operator, which are derived from the one-loop calculation with data set 2 and $B_0 = 1.3914 \times 10^2 [\text{MeV}]$. The first column corresponds to the operator number of the effective Hamiltonian (3.29) and (3.30). The second row shows the observed data.

S-wave:

vertex	Σ_-^-	Σ_+^+	Σ_0^+	Λ_0^0	Λ_-^0	Ξ_-^-	Ξ_0^-
exp.	1.93	0.06	-1.48	-1.07	1.47	-2.04	-1.54
O_1	0.8109	0.03720	-0.5395	-0.7886	1.124	-1.212	0.8587
O_2	0.06608	0.003031	-0.04396	-0.06425	0.09157	-0.09876	0.06996
O_3	0.1346	0.004306	-0.09025	-0.06023	0.08568	-0.1685	0.1178
O_4	0.3988	-0.08284	0.4980	0.4776	0.3318	-0.3530	-0.4974
O_{51}	0	0	0	0	0	0	0
O_{52}	-0.02663	0	0.01884	0.1102	-0.1558	0.05705	-0.04033
O_{53}	-0.06330	0.002354	0.04215	0.03044	-0.04338	0.06150	-0.04172
O_{61}	0.7101	-0.0002238	-0.5023	-2.938	4.156	-1.521	1.075
O_{62}	1.688	-0.06277	-1.124	-0.8116	1.157	-1.640	1.113

P-wave:

vertex	Σ_-^-	Σ_+^+	Σ_0^+	Λ_0^0	Λ_-^0	Ξ_-^-	Ξ_0^-
exp.	-0.65	19.07	12.04	-7.14	9.98	6.93	-6.43
O_1	0.5634	6.890	4.473	-1.549	2.191	0.007857	-0.005556
O_2	0.05174	0.5680	0.3650	-0.1240	0.1753	0.005649	-0.003995
O_3	0.06527	-0.2370	-0.2137	0.1996	-0.2822	-0.1340	0.09473
O_4	1.028	-0.004212	1.450	0.5049	0.3570	-0.2686	-0.3799
O_{51}	-3.976E-4	-4.487E-4	-3.612E-5	-1.561E-4	2.207E-4	-3.415E-4	2.415E-4
O_{52}	-0.8817	-0.7550	0.08955	-1.337	1.892	-0.8356	0.5909
O_{53}	0.9487	0.3746	-0.4058	1.515	-2.143	0.8626	-0.6098
O_{61}	23.51	20.13	-2.388	35.67	-50.44	22.28	-15.76
O_{62}	-25.30	-9.990	10.82	-40.39	57.13	-23.00	16.26

Table 4.7 The S- and P-wave $\Delta I = 3/2$ amplitudes of each decay mode. The second column shows the experimentally obtained ratio of $\Delta I = 3/2$ and $\Delta I = 1/2$ amplitudes. The third column represents the $\Delta I = 3/2$ amplitudes which are calculated with the total decay amplitude and the ratio of the second column. The fourth and fifth column show the $\Delta I = 3/2$ amplitude obtained by the effective weak Hamiltonian (3.29).

S-wave

decay mode	$A^{3/2}/A^{1/2}$	$A_{exp.}^{3/2}$	$A_{tree}^{3/2}$	$A_{tree+loop}^{3/2}$
Σ_{-}^{-}	-0.061 ± 0.024	-0.1254	0.06909	0.4679
Σ_{+}^{+}	-0.061 ± 0.024	-0.003898	0.0	-0.08284
Σ_{0}^{+}	-0.061 ± 0.024	0.09614	0.09770	0.5957
Λ_{0}^{0}	0.027 ± 0.008	-0.02813	0.08735	0.5650
Λ_{-}^{0}	0.027 ± 0.008	0.03865	0.06176	0.3936
Ξ_{-}^{-}	-0.038 ± 0.014	0.08058	-0.06978	-0.4228
Ξ_{0}^{0}	-0.038 ± 0.014	-0.06083	-0.09868	-0.5961

P-wave

decay mode	$B^{3/2}/B^{1/2}$	$B_{exp.}^{3/2}$	$B_{tree}^{3/2}$	$B_{tree+loop}^{3/2}$
Σ_{-}^{-}	-0.074 ± 0.027	0.05194	0.1368	1.165
Σ_{+}^{+}	-0.074 ± 0.027	-1.524	0.0	-0.004212
Σ_{0}^{+}	-0.074 ± 0.027	-0.9622	0.1935	1.644
Λ_{0}^{0}	0.030 ± 0.037	-0.2080	-0.6759	-0.1710
Λ_{-}^{0}	0.030 ± 0.037	0.2907	-0.4779	-0.1209
Ξ_{-}^{-}	-0.17 ± 0.09	-1.419	0.1853	-0.0833
Ξ_{0}^{0}	-0.17 ± 0.09	1.317	0.2621	-0.1178

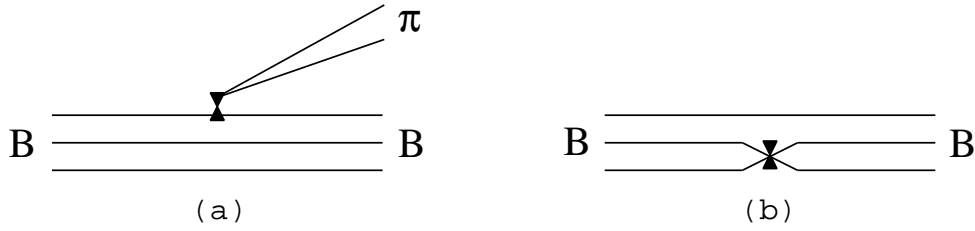


Figure 3.1: $\Delta S = 1$ hyperon non-leptonic weak decay of quark currents. (a) corresponds to the weak interaction between two hadronic currents which are color singlet. (b) corresponds to the weak interaction inside the hyperon.

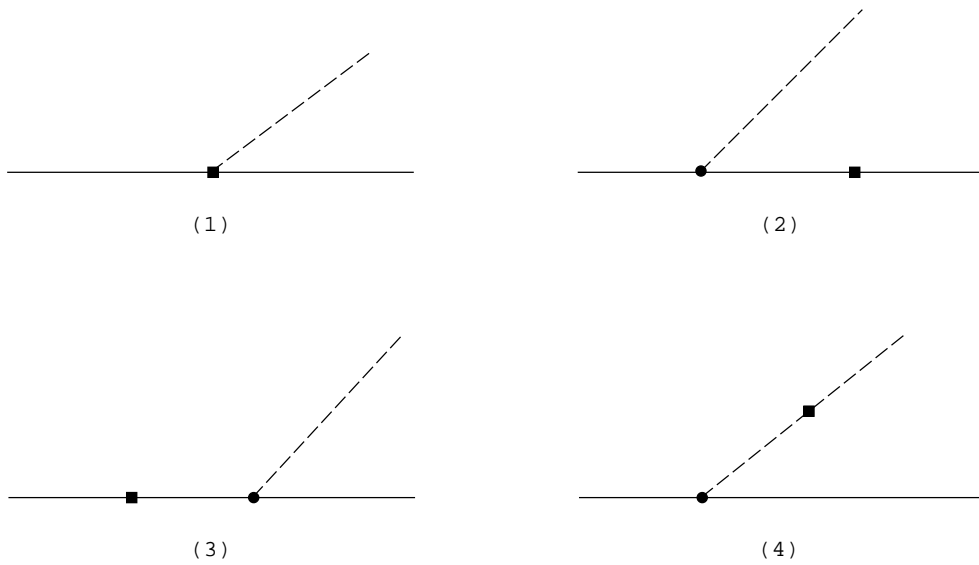


Figure 4.1: Tree graph for hyperon non-leptonic decay. Single solid lines represent octet baryon fields and dots lines represent meson fields. The solid square denotes $\Delta S = 1$ weak interaction vertices and the solid dot denotes strong interaction vertices.

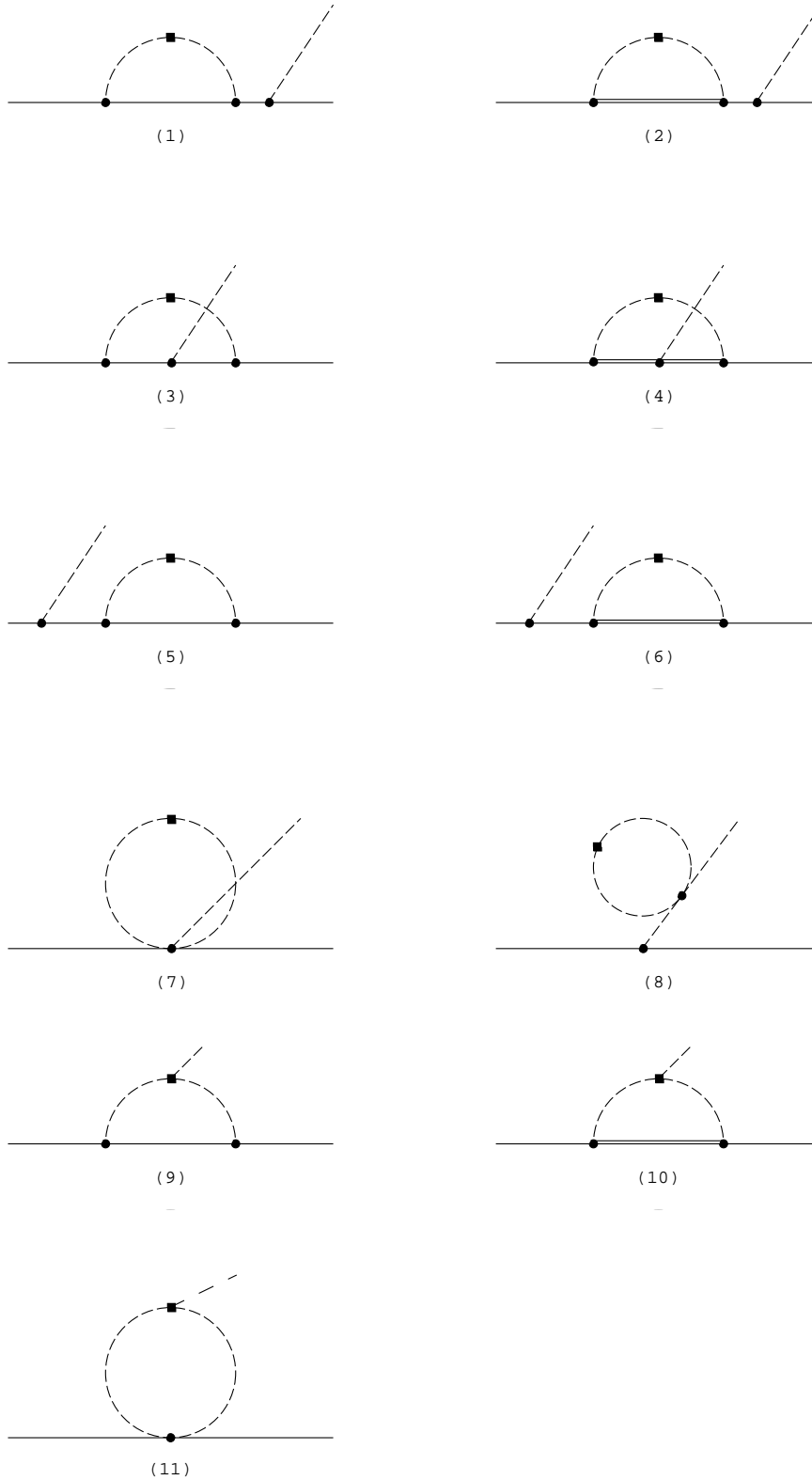


Figure 4.2: One loop diagrams for hyperon non-leptonic weak decay. Single solid lines represent octet baryon fields, double solid lines represents decuplet fields and dots lines denote meson fields. the solid square denotes $\Delta S = 1$ weak interaction vertices and the solid dot denotes strong interaction vertices.

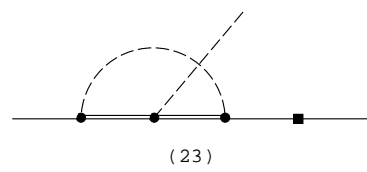
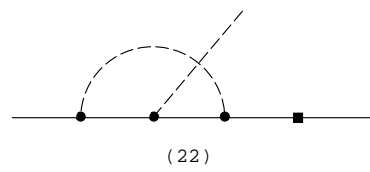
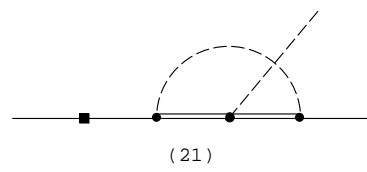
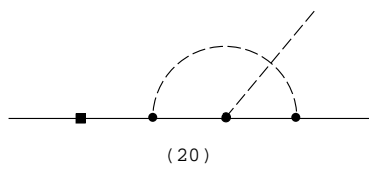
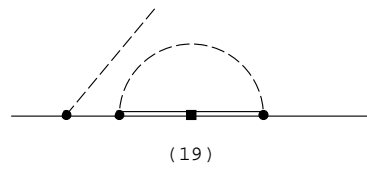
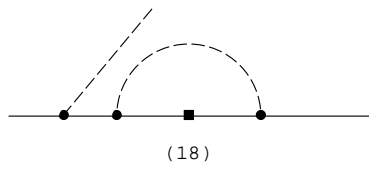
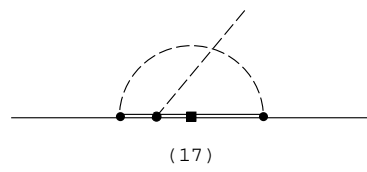
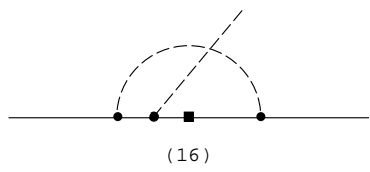
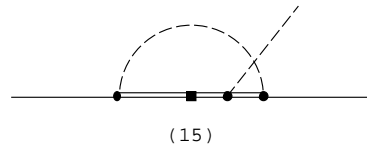
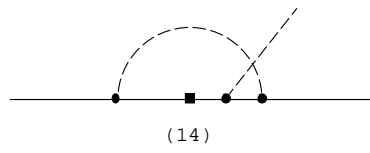
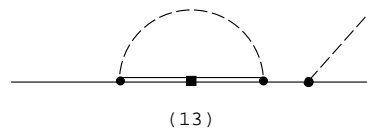
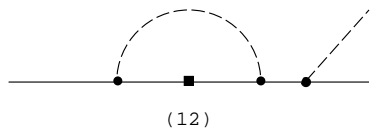


Figure 4.2: (continued)

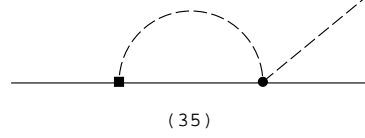
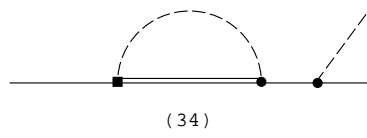
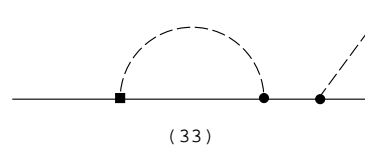
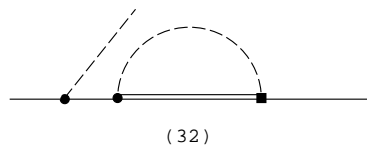
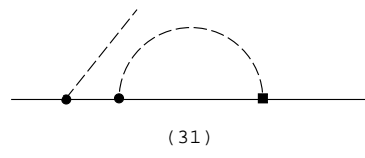
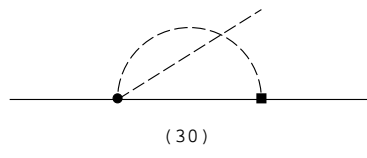
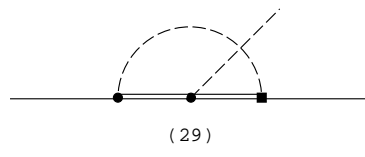
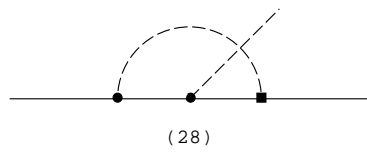
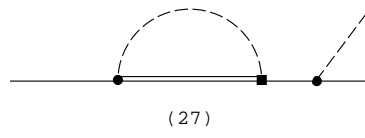
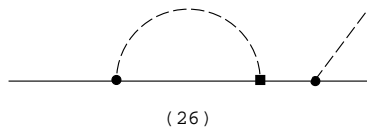
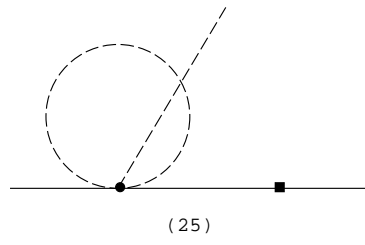
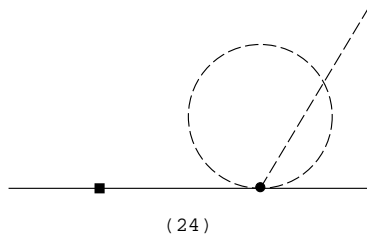


Figure 4.2: (continued)

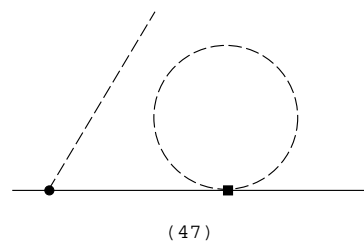
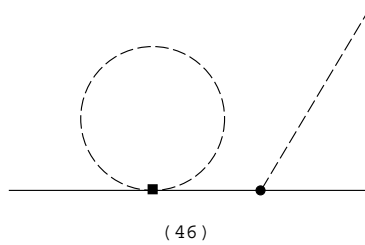
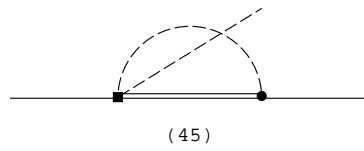
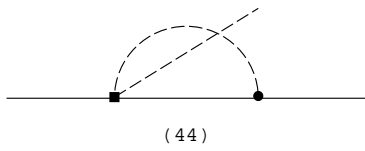
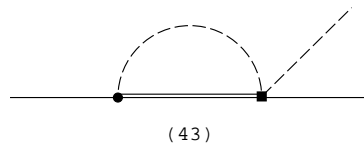
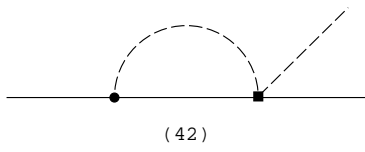
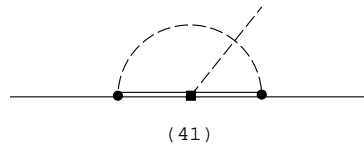
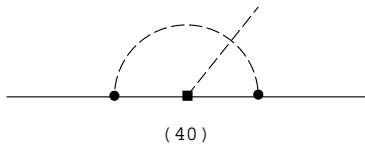
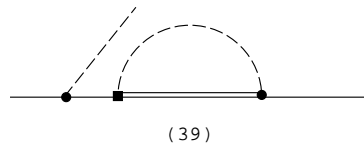
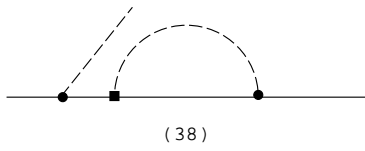
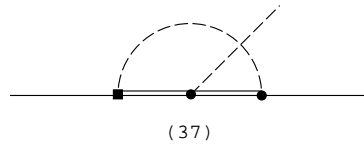
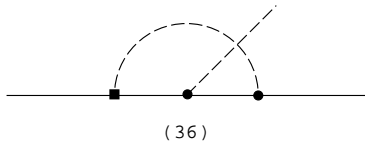


Figure 4.2: (continued)



Figure 4.2: (continued)

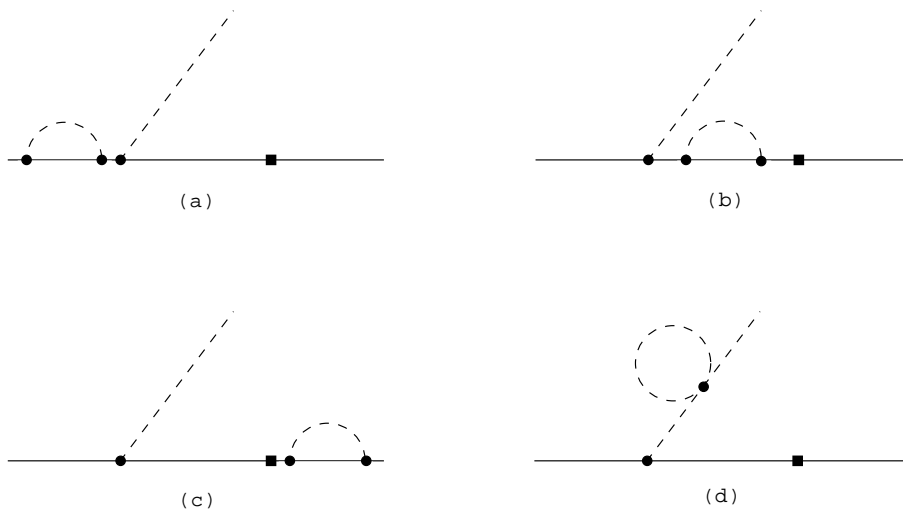


Figure 4.3: Examples of the wave function renormalization applied to the tree diagram in Figure 4.2 (2). In this study, it is considered that the internal baryon state is the decuplet baryon.